AMERICAN SOCIETY FOR MICROBIOLOGY | Journal of Virology

A Proline-Rich N-Terminal Region of the Dengue Virus NS3 Is Crucial for Infectious Particle Production

Leopoldo G. Gebhard, Néstor G. Iglesias, Laura A. Byk, Claudia V. Filomatori, Federico A. De Maio, Andrea V. Gamarnik

Fundación Instituto Leloir and Consejo Nacional de Investigaciones Científicas y Técnicas (CONICET), Buenos Aires, Argentina

ABSTRACT

Dengue virus is currently the most important insect-borne viral human pathogen. Viral nonstructural protein 3 (NS3) is a key component of the viral replication machinery that performs multiple functions during viral replication and participates in antiviral evasion. Using dengue virus infectious clones and reporter systems to dissect each step of the viral life cycle, we examined the requirements of different domains of NS3 on viral particle assembly. A thorough site-directed mutagenesis study based on solvent-accessible surface areas of NS3 revealed that, in addition to being essential for RNA replication, different domains of dengue virus NS3 are critically required for production of infectious viral particles. Unexpectedly, point mutations in the protease, interdomain linker, or helicase domain were sufficient to abolish infectious particle formation without affecting translation, polyprotein processing, or RNA replication. In particular, we identified a novel proline-rich N-terminal unstructured region of NS3 that contains several amino acid residues involved in infectious particle formation. We also showed a new role for the interdomain linker of NS3 in virion assembly. In conclusion, we present a comprehensive genetic map of novel NS3 determinants for viral particle assembly. Importantly, our results provide evidence of a central role of NS3 in the coordination of both dengue virus RNA replication and particle formation.

IMPORTANCE

Dengue virus is an important human pathogen, and its prominence is expanding globally; however, basic aspects of its biology are still unclear, hindering the development of effective therapeutic and prophylactic treatments. Little is known about the initial steps of dengue and other flavivirus particle assembly. This process involves a complex interplay between viral and cellular components, making it an attractive antiviral target. Unpredictably, we identified spatially separated regions of the large NS3 viral protein as determinants for dengue virus particle assembly. NS3 is a multifunctional enzyme that participates in different steps of the viral life cycle. Using reporter systems to dissect different viral processes, we identified a novel N-terminal unstructured region of the NS3 protein as crucial for production of viral particles. Based on our findings, we propose new ideas that include NS3 as a possible scaffold for the viral assembly process.

The dengue virus (DENV) belongs to the *Flavivirus* genus of the *Flaviviridae* family, together with other important emerging and reemerging human pathogens, such as Zika virus (ZKV), West Nile virus (WNV), Japanese encephalitis virus (JAEV), Saint Louis encephalitis virus (SLEV), yellow fever virus (YFV), and tick-borne encephalitis virus (TBEV) (1–3). DENV comprises four closely related serotypes (DENV-1 to -4), and all of them can produce disease ranging from mild dengue fever to severe dengue, a potentially lethal hemorrhagic and capillary leak syndrome. Found in tropical and subtropical regions of the world, dengue is the most significant viral disease transmitted by arthropods. It is estimated to cause 390 million infections per year and places over 3 billion people at risk of infection (4). In spite of this great burden, fundamental aspects of its viral biology remain elusive, and effective therapeutics are still unavailable (5).

The flavivirus genome is a single RNA molecule of about 11 kb that carries one open reading frame (ORF), flanked by highly structured 5′ and 3′ untranslated regions (UTRs). The single polyprotein is processed co- and posttranslationally to give three structural proteins (capsid [C], premembrane protein [prM], and envelope [E]) and seven nonstructural proteins (NS1, NS2A, NS2B, NS3, NS4A, NS4B, and NS5). The structural proteins integrate the viral particle, while the nonstructural proteins support replication of the viral RNA and virion assembly and limit the host antiviral response (6–11). Although great advances have been made in recent years to understand the mechanism of viral genome replication (12–16), less is known about the process that leads to genome encapsidation during viral assembly (17–20).

Viral particle formation requires the assembly of a nucleocapsid integrated by the viral genome and multiple copies of the C protein. The process of genome recruitment by C has been proposed to take place near RNA replication complexes associated with endoplasmic reticulum (ER) membranes (18, 21); however, the specifics of the viral and cellular components of the assembly machinery are still unclear, as are the mechanistic details of how it works. A number of reports have involved the NS1, NS2A, and NS3 flavivirus proteins as components of this machinery (22–27), but how the interplay between these components and the host cell

Received 2 February 2016 **Accepted** 17 March 2016

Accepted manuscript posted online 23 March 2016

Citation Gebhard LG, Iglesias NG, Byk LA, Filomatori CV, Maio FAD, Gamarnik AV. 2016. A proline rich N-terminal region of the dengue virus NS3 is crucial for infectious particle production. J Virol 90:5451–5461. doi:10.1128/JVI.00206-16.

Editor: M. S. Diamond, Washington University School of Medicine

Address correspondence to Andrea V. Gamarnik, agamarnik@leloir.org.ar.

Supplemental material for this article may be found at http://dx.doi.org/10.1128/JVI.00206-16.

occurs remains uncertain. Using YFV, a genetic link was first uncovered between NS2A and NS3 for viral particle assembly. A mutation in NS2A that impairs particle formation was rescued by a second site mutation in NS3 (22). Further analysis confirmed an assembly requirement of specific residues in the helicase domain of YFV NS3 protein (23). NS3 is a multifunctional protein with activities involved in polyprotein processing, viral RNA replication, and host immune evasion (20, 28–39). The protein bears an N-terminal serine protease domain (residues 1 to 169) and a C-terminal region containing RNA helicase, nucleoside triphosphatase (NTPase), 5′-RNA triphosphatase (RTPase), and RNA annealing activities (residues 179 to 618) (32, 40–42). Because of its essential role early in polyprotein processing and RNA replication, genetic studies thus far have provided limited information on the molecular determinants of NS3 responsible for assembly and release of infectious virus particles.

Here, we used a DENV reporter system that allows the dissecting of each step of the viral life cycle to investigate the involvement of DENV NS3 in viral particle assembly. A systematic mutagenesis study taking into account three-dimensional structures of NS3 and its individual domains, as well as solvent-accessible surface areas, identified novel determinants for DENV particle assembly.

MATERIALS AND METHODS

Cell culture. Baby hamster kidney cells (BHK-21) were maintained in minimum essential medium (MEM) alpha supplemented with 10% fetal bovine serum (FBS), 100 U/ml penicillin, and 0.10 mg/ml streptomycin (Gibco). Cells were grown in an incubator at 37°C and 5% CO_2.

Plasmids. Monocistronic dengue virus reporter construct (mDV-R) containing the *Renilla* luciferase (Rluc) coding sequence was previously described (43). This construct contains the Rluc reporter gene just downstream of the minimal *cis*-acting elements (MCAE) of the viral ORF, followed by an FMDV-2A autoproteolytic protease sequence in order to release the Rluc enzyme from the viral polyprotein. A plasmid containing the DENV-2 strain 16681 infectious cDNA clone also was used (GenBank accession number U87411) (44).

Cloning and site-directed mutagenesis. The desired mutations within the coding sequence of NS3 were introduced into the mDV-R cDNA clone by replacing the KpnI-NsiI, NsiI-XhoI, or XhoI-NheI fragment of the wild-type (WT) plasmid with the respective fragment derived from overlapping PCR using primers listed in Table S1 in the supplemental material. Selected NS3 mutations were also introduced in the plasmid containing the DENV-2 16681 infectious clone by double digestion and T4 DNA ligation of the respective mDV-R clone. *Pfu* DNA polymerase was obtained from FIL. Restriction enzymes, T4 DNA ligase, and Antarctic phosphatase were purchased from New England BioLabs Inc. DNA sequences were confirmed by automatic DNA sequencing using a 3130 genetic analyzer (Applied Biosystems).

RNA transcription. Plasmids were linearized with XbaI and used as transcription templates. DENV genomic RNAs were obtained by *in vitro* transcription using T7 RNA polymerase (Ambion) in the presence of an $m^7G(5')ppp(5')A$ RNA Cap structure analog (S1405L; New England BioLabs Inc.) as previously described (45). In cases where transfected cells were used in quantitative real-time reverse transcription-PCR (RT-qPCR), the DNA templates were removed from the reaction mix by digestion with Turbo DNase (Ambion). RNA integrity was confirmed by agarose gel electrophoresis.

RNA transfections with reporter virus RNAs. RNA transfections were performed with Lipofectamine 2000 according to the manufacturer's instructions (Invitrogen). BHK cells were seeded in 24-well plates at a density of $\sim 4 \times 10^4$ cells per well. The next day, the semiconfluent (~70%) cellular monolayers were transfected with 500 ng per well of mDV-R RNA transcripts. After 3 h of incubation, RNA/Lipofectamine fluids were removed and replaced with 0.5 ml of fresh culture medium. The Rluc activity present in mDV-R-transfected cells was analyzed at 6, 24, 48, and 72 h posttransfection (hpt) from cell extracts using the *Renilla* luciferase assay system according to the manufacturer's instructions (Promega). Each reporter virus was assayed in two separated wells for every time point measured. At least three independent experiments were performed for each virus. The supernatant fluids from respective wells at 72 hpt were collected and stored at −70°C for subsequent release infectivity analysis. WT, replication-defective (NS5), and encapsidation-defective (ΔC) reporter viruses were added as controls to these assays (43, 46).

Release infectivity assay of reporter virus. In order to quantify the release infectivity for each NS3 mutant of the reporter virus, these supernatants were thawed and applied (0.2 ml/well) to naive BHK cells grown under the same conditions described above. The Rluc activity present in the infected cells was analyzed from cell extracts at 1 and 3 days postinfection (dpi) using the *Renilla* luciferase assay system (Promega).

IFA. For indirect immunofluorescence assay (IFA), BHK cells were seeded into 24-well plates containing glass coverslips. The next day, the cells grown at ~70% confluence were transfected as described above with WT DENV-2 infectious clone RNA and selected NS3 mutants that solely impaired virus propagation in the reporter virus. At 2 days posttransfection, supernatant fluids were harvested and stored at −70°C, while coverslips were collected and the cells were fixed with 4% paraformaldehyde, 4% sucrose in phosphate-buffered saline (PBS), pH 7.4, at room temperature for 15 min. Coverslips were washed with PBS, and then fixed cells were permeated with 0.1% Triton X-100 for 4 min at room temperature. For the detection of DENV-infected cells, mouse monoclonal anti-E antibody E18 (dilution of 1:200 in PBS with 0.2% gelatin) was used (47). Secondary staining was carried out using a 1:500 dilution of Alexa 488-conjugated anti-mouse IgG antibody (Invitrogen Inc.). Nuclear DNA was stained with a 1:1,000 dilution of 4′,6-diamidino-2-phenylindole (DAPI) (Molecular Probes, Karlsruhe, Germany). Coverslips were mounted with Mowiol 4-88 (Sigma). Images were obtained with a Carl Zeiss AXIO Imager.A2 fluorescence microscope at ×100 magnification. The supernatant fluids collected at 2 days posttransfection were thawed and applied to naive BHK cells. After 1 and 4 days postincubation, DENV-infected cells (green fluorescence) were analyzed by IFA in order to estimate the release infectivity for each virus.

WB. For Western blotting (WB) assays, the following antibodies and antisera were used. The immunodetection of E was performed using the specific monoclonal antibody E18 (47). Rabbit polyclonal anti-capsid serum was obtained previously (43). Rabbit polyclonal anti-NS3 serum was obtained in our laboratory. The specificity of this antiserum was evaluated by enzyme-linked immunosorbent assay (ELISA) and Western blotting employing DENV-infected and noninfected BHK cell extracts as controls. Mouse monoclonal anti-glyceraldehyde-3-phosphate dehydrogenase (GAPDH; 6C5) was used for a loading control (Abcam). Horseradish peroxidase (HRP)-conjugated donkey anti-mouse IgG and HRP-conjugated goat anti-rabbit IgG sera were used as secondary antibodies (Sigma).

For the detection of intracellular C, NS3, E, and GAPDH, BHK cells were grown in 24-well plates and transfected with the WT and mutant DENV-2 infectious clone as described above. At 2 and 3 days posttransfection, supernatant fluids were recovered and store on ice, while transfected cells were suspended by trypsinization, washed once with PBS supplemented with 2% FBS, and then washed twice with PBS. Cells were pelleted and stored at −70°C. Cells were thawed and denatured in buffer S (1% sodium dodecyl sulfate [SDS], 10 mM Tris, pH 6.8, and 5% glycerol) at 95°C for 5 min. Samples were analyzed under denaturing conditions by SDS-PAGE, transferred to Amersham Hybond P polyvinylidene difluoride (PVDF) membranes (0.45-μm pore size; GE-Healthcare Life Sciences), and blocked overnight with 5% low-fat milk in TBS–0.1% Tween 20 at 4°C, and Western blot analyses were performed using the specific antibodies mentioned above. For the detection of secreted E and C protein in transfected cells, supernatant fluids obtained 2 and 3 dpt were

centrifuged at 4°C for 15 min at 15,000 × *g* to clear cellular debris. Aliquots of 50 μl were denatured and analyzed by WB as described above.

RNA extraction, reverse transcription, and real-time PCR. The intracellular extracts and supernatant fluids of cells transfected with WT or NS3-mutated viruses were obtained as described above. Total RNA from samples was extracted with TRIzol by following the manufacturer's recommendations (Invitrogen). RNA extracted from experimental samples was reverse transcribed in 20-μl reaction volumes using 160 U Moloney murine leukemia virus (M-MLV) RT (Promega), 4 U of RNasin RNase inhibitors (Promega), 500 nM primer AVG1118 (5′-GCCGCACCATTG GTCTTCTC-3′), and 0.5 mM each deoxynucleoside triphosphate (dNTP), all in 1× M-MLV RT buffer. Primer and RNA template were preincubated for 5 min at 70°C. The RT reaction was allowed to proceed for 1 h at 42°C and then for 15 min at 65°C to denature the RT enzyme. For quantitative real-time PCR, an Mx3005P qPCR system (Agilent Technologies Inc.) was employed. Reactions were performed in triplicate in 96-well plates using 2 μl of the RT reaction as the template (1:10 dilution in RNase-free water), 5 μl FastStart Universal SYBR green master (Rox) 2× mix (Roche), 300 nM each primer, and RNase-free water to 10 μl. The primers AVG1117 (5′-ACAAGTCGAACAACCTGGTCCAT-3′) and AVG1118 were targeted to amplify nucleotides 9937 to 10113 within the NS5 coding sequence. Reactions were run with the following parameters: 95°C for 15 min and then 40 cycles of 95°C for 10 s and 60°C for 30 s. Fluorescence detection was acquired during the elongation step of each cycle. For each reaction the initial amount of template was calculated from the threshold cycle (C_T) value using a standard curve generated from serial dilutions of reverse-transcribed and purified genomic RNA.

Virus plaque- and focus-forming assays. Supernatant fluids from WT and NS3 mutant DENV-transfected cells were harvested at 3 days posttransfection and stored at −70°C. These fluids were used to infect fresh cells in order to quantify viral titers. Viral titers were quantified by plaque titration assay as described previously (45). Briefly, supernatant fluids were serially diluted, added to fresh cells in 24-well plates, and incubated for 1 h. Afterwards, 1 ml of overlay medium (culture medium supplemented with 0.8% methyl cellulose) was added to each well. Cells were fixed 7 days postincubation by addition of 0.5 ml 10% formaldehyde per well, incubated for 1 h, thoroughly washed with water, and stained with crystal violet. For the focus-forming assay, supernatant fluids were serially diluted, and 0.20 ml was added to fresh cells grown in 24-well plates and incubated for 1 h. Afterwards, 1 ml of overlay medium was added to each well. At 5 days postincubation, overlays were washed away and cells were fixed with 0.5 ml methanol for 20 min at 4°C. Fixed cells were washed with Tris-buffered saline (TBS), pH 7.4, and incubated for 2 h in blocking buffer (TBS supplemented with 0.25 mM EDTA, 1% BSA, and 0.1% Tween 20). Two hundred microliters of mouse monoclonal anti-E antibody E18 (1:500 dilution in blocking buffer) then was added to each well and incubated for 1 h at room temperature. After three washes with blocking buffer, 200 μl alkaline phosphate-conjugated anti-mouse IgG antibody (1:2,500 dilution in blocking buffer) was added and incubated for 1 h. After thorough washes with TBS, BCIP-NBT (5-bromo-4-chloro-3-indolylphosphate–nitroblue tetrazolium) color development substrate was added as indicated by the manufacturer (Promega).

RESULTS AND DISCUSSION

Based on the X-ray crystal structure determined for the DENV-2 NS3hel domain (PDB code 2BMF [48]), the solvent-accessible surface area for each amino acid residue was computed using the GetArea program (49). Residues with side chains that point away from the NS3hel core domain were identified. Amino acids within known functional/conserved motifs for enzymatic activities were excluded (34). Double or triple mutations to alanine of contiguous (or very close) solvent-exposed residues were tested. Additionally, mutant $W_{344}A$, corresponding to the homologue $W_{349}A$ substitution previously identified in the NS3hel of YFV as relevant for viral assembly (23), was included in the analysis (Fig. 1A). A ribbon diagram representation of the NS3 protein structure indicating the 3D location of the selected residues was generated using Pymol (DeLano Scientific) (Fig. 1B).

We designed and constructed six recombinant viruses with mutations in the NS3hel domain and assessed replication and infectivity using a *Renilla* luciferase reporter DENV-2 (mDV-R), competent for replication and production of infectious particles (43, 46). Mutations were introduced in the cDNA clone by overlapping PCR (using primers listed in Table S1 in the supplemental material). RNA transcriptions and transfections were carried out as previously reported (43, 46). Measurements of luciferase activity expressed from the mDV-R RNA-transfected cells were performed at 6, 24, 48, and 72 hpt. The first rounds of RNA translation were evaluated at 6 h and RNA replication at 24, 48, and 72 h (Fig. 1C). Four controls were used, the parental viral RNA (WT), a replication-impaired RNA with a mutation in the viral polymerase (NS5), a propagation-impaired control with a deletion of the capsid protein (ΔC), and a mock transfection. To examine secreted infectious particles, the culture supernatants from each case were collected at 72 h and used to infect fresh BHK-21 cells, and luciferase was monitored as a function of time postinfection (Fig. 1D). As expected, transfection of the WT reporter virus RNA resulted in efficient viral replication and production of infectious viral particles (Fig. 1C and D, WT). The replication control (NS5) showed high levels of translation (6 h) but no RNA amplification, while the ΔC control showed WT levels of translation and RNA replication but undetectable infectious particles (Fig. 1C and D, NS5 and ΔC). All of the mutations introduced in NS3hel diminished viral replication to some extent (Fig. 1C). In contrast to that observed in YFV, alteration of the homologous and conserved tryptophan residue to alanine ($W_{344}A$) in DENV NS3hel resulted in a drastic reduction of viral replication, and consequently an undetectable production of viral particles, indicating a different requirement for the replication/assembly machinery of these two related viruses (Fig. 1C and D, $W_{344}A$). The triple-residue mutant $P_{501}A+E_{502}A+I_{504}A$ showed a drastic reduction in replication, comparable to the profile obtained for the NS5 control, suggesting that these residues were crucial for RNA amplification. Mutants $V_{273}A+R_{274}A+P_{276}A$, $K_{213}A+R_{214}A$, and $R_{526}A+E_{528}A+K_{531}A$ presented significant reduction in viral replication at different degrees (Fig. 1C). As a consequence of these defects in replication, a major reduction or impediment in virus infectivity was observed for these three mutants (Fig. 1D).

The mutation $E_{574}A+E_{575}A+N_{576}A$ produced only a slight delay in viral replication. At 72 h posttransfection, the luciferase activity was similar to that observed for the WT (Fig. 1C). Notably, this substitution drastically decreased the production of infectious viral particles (>10,000-fold less than that for the WT) (Fig. 1D). Alignments using sequences from different flaviviruses revealed that these amino acids are highly conserved (Fig. 1E). To further examine the possible relevance of these residues on viral particle assembly, they were individually mutated in the reporter virus. Translation and replication of the three mutants carrying each single substitution ($E_{574}A$, $E_{575}A$, or $N_{576}A$) were indistinguishable from the WT (Fig. 1F). Interestingly, while mutant $E_{575}A$ produced a moderate reduction in infectivity (10-fold reduction of Rluc activity at 3 dpi), the $N_{576}A$ mutation greatly reduced (more than 1,000-fold) the production of infectious particles (Fig. 1G). These results indicate that the conserved residue N_{576}, located at subdomain III of NS3hel, performs an important function

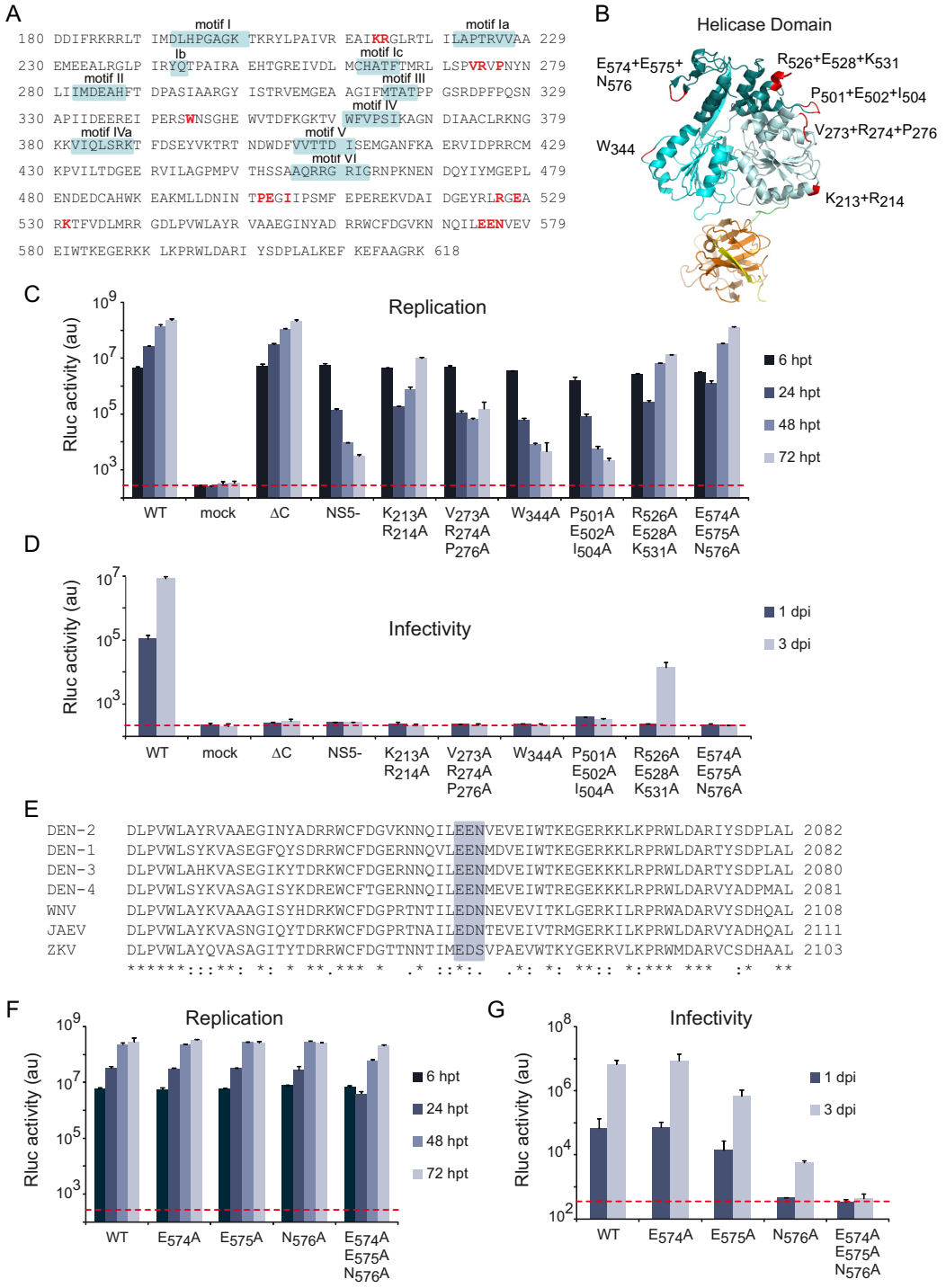

FIG 1 DENV helicase domain of NS3 is involved in infectious particle production. (A) Sequence of DENV-2 NS3 helicase domain (residues 180 to 618) of strain 16681 is shown, with the helicase superfamily 2 conserved motifs in boxes and the amino acids involved in the mutagenesis analysis in red. (B) Ribbon diagram representation of the X-ray crystal structure of the DENV NS3 protein (PDB accession number 2VBC) (52). The helicase domain is formed by three subdomains (shown in bluish tones). The protease domain is formed by the N-terminal third of the NS3 polypeptide with part of NS2B cofactor (shown in orange and yellow, respectively). The interdomain *linker* region (residues 170 to 179) is shown in green. Residues targeted by site-directed mutagenesis are indicated in red. (C) Translation and replication levels of the *Renilla* luciferase (Rluc) reporter system mDV-R containing the engineered mutations in the helicase domain of NS3. Rluc activity was measured at the indicated times in transfected cells with viral RNAs corresponding to the WT reporter virus, the replication-impaired NS5 mutant, the propagation-impaired ΔC mutant, and the engineered NS3 mutant. Data correspond to the averages from three independent experiments. Error bars point out standard deviations. The red dashed line indicates background levels of the signal. au, arbitrary units. (D) Released infectivity from mDV-R-transfected cells. Culture supernatants (0.25 ml) collected at 72 hpt from transfected cells shown in panel C were used to inoculate fresh cells, and then luciferase activity in these cells was measured at 1 and 3 days postincubation. (E) Multiple-sequence alignment of N_{576} and surrounding residues of the NS3 proteins from the four DENV serotypes and other flaviviruses. The triple mutation of the solvent-accessible conserved residues E_{574}, E_{575}, and N_{576} (shaded blue) for alanine abrogates the release infectivity of reporter virus. Asterisks, colons, and dots indicate identical, conserved, and partially conserved residues, respectively. (F) Translation and replication levels in RNA-transfected BHK-21 cells of the reporter virus carrying single-residue mutations of E_{574}A, E_{575}A, and N_{576}A. WT and triple-mutant data are also included for ease of comparison. (G) Released infectivity assays of the culture supernatants collected at 72 h posttransfection from each mutant shown in panel F.

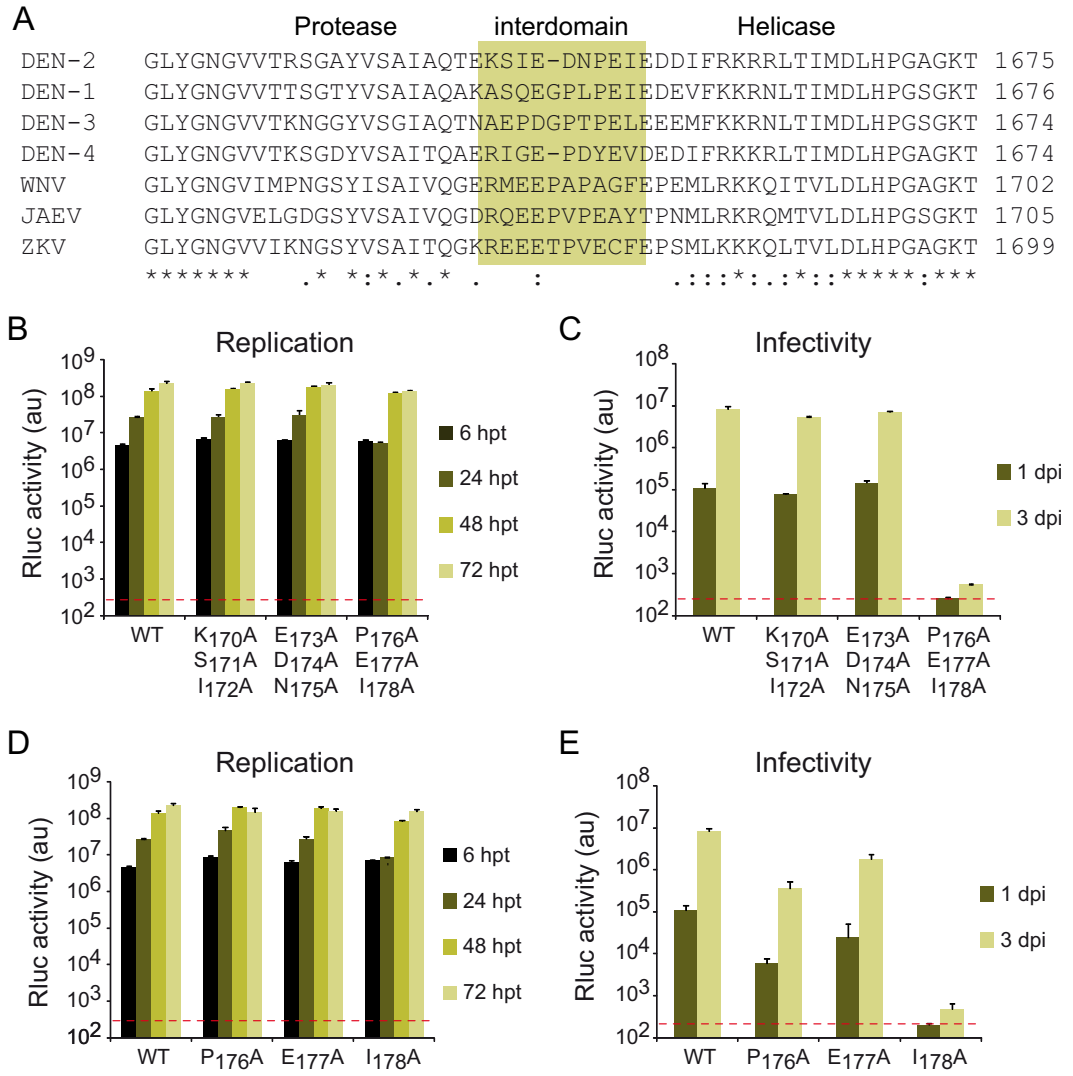

FIG 2 Identification of the linker region that tethers the protease and the helicase domains of NS3 as a critical determinant for DENV propagation. (A) Multiple-sequence alignment of the NS3 interdomain region from the four DENV serotypes and other flaviviruses. Based on the available structure of full-length NS3 comprising both protease and helicase domains from DENV-4, we demarcate the interdomain linker region (highlighted in light brown). (B) Translation and replication capabilities of the reporter viruses containing mutations in the linker region of the NS3 protein were assayed as described for Fig. 1. The WT was also included for ease of comparison. The dashed line indicates background levels of luciferase activity. (C) Released infectivity measurements of the culture supernatants collected at 72 h posttransfection from DV-R RNA-transfected cells shown in panel B. (D) Translation and replication capabilities of the reporter viruses carrying single-residue mutations of $P_{176}A$, $E_{177}A$, and $I_{178}A$ in DV-R-transfected cells. (E) Released infectivity measurements at the indicated time after transfection of the culture supernatants collected from cell cultures shown in panel D at 72 h posttransfection.

in viral assembly without reducing the enzymatic activities involved in the first steps of the viral life cycle.

The linker region (residues 170 to 178 in NS3 of DENV-2) that naturally tethers the protease and helicase domains is particularly interesting because it allows NS3 to acquire different conformations relevant for the diverse functions of the protein (50, 51). It has been reported that increasing the linker flexibility led to a significant reduction in the ATPase and helicase activities *in vitro* and a decrease in viral RNA replication in cell culture (50). Crystallographic studies carried out with the DENV-4 NS3 solved two structures for the same protein crystallized under different conditions (50, 52). In both cases the protease and helicase domains were superimposed separately as independent entities, and their structures were consistent with those previously obtained for the isolated protease and helicase domains (48, 50, 53). Interestingly, while the full-length NS3 molecule adopted elongated shapes in both conformations, they diverged in a 161° rotation between the domains, which correlated with a reorientation of segment E_{177}-D_{179} in the linker (50). Based on the structural/functional relevance of this linker region, we performed a systematic mutational analysis to assess its possible involvement in viral assembly.

Sequence alignments of the NS3 interdomain region obtained from the four DENV serotypes was found not to be well conserved (Fig. 2A). Three triple-residue substitutions comprising the complete linker first were designed in the context of DENV-2 (Fig. 2B and C). Mutants $K_{170}A+S_{171}A+I_{172}A$ and $E_{173}A+D_{174}A+N_{175}A$ exhibited replication and infectivity levels similar to those of the WT, whereas mutant $P_{176}A+E_{177}A+I_{178}A$ showed a very slight

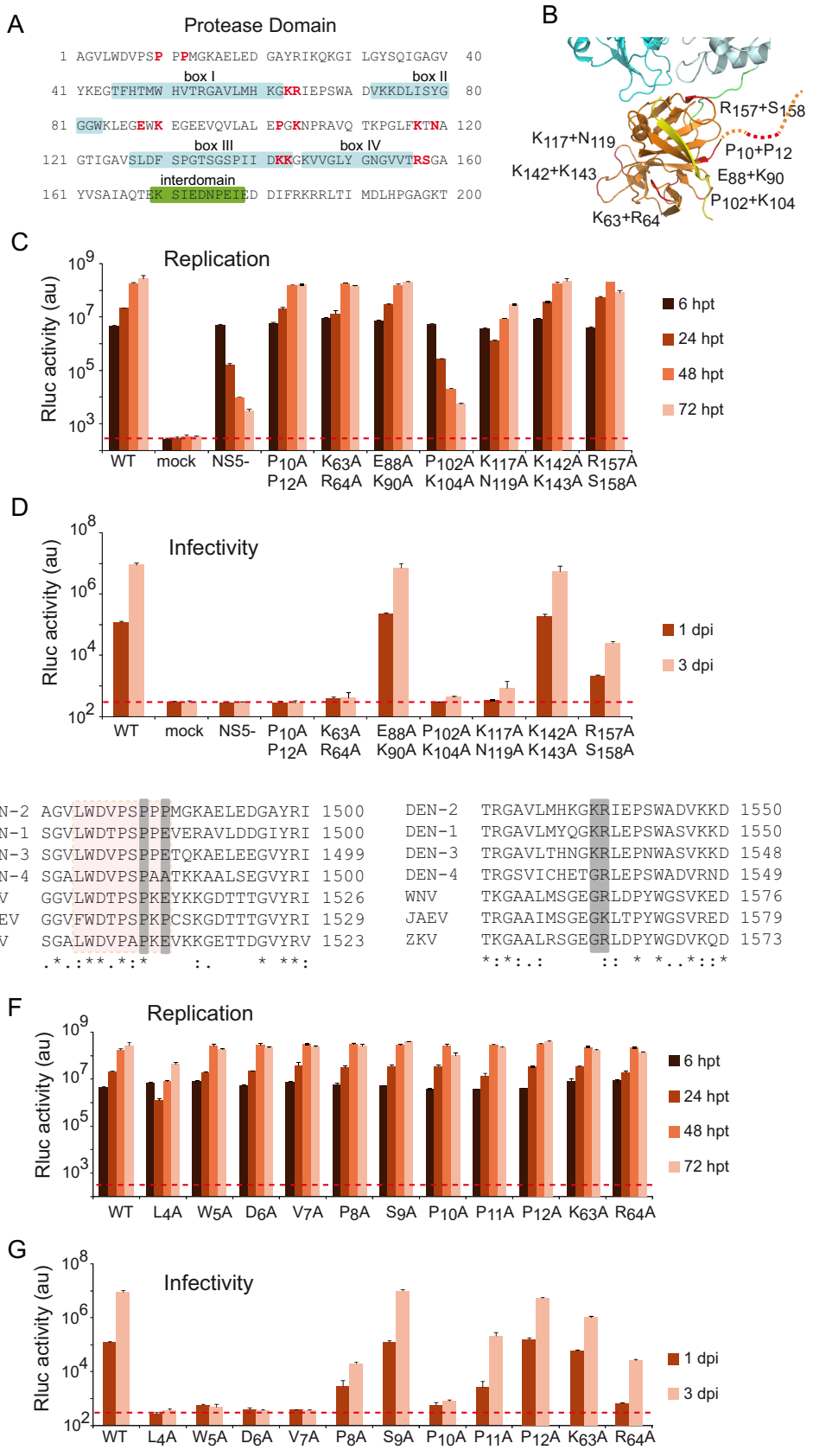
A
Protease Domain
box I
box II
box III
box IV
interdomain
B
C
Replication
Rluc activity (au)
6 hpt
24 hpt
48 hpt
72 hpt
WT
mock
NS5-
D
Infectivity
1 dpi
3 dpi
E
F
G

delay in replication (Fig. 2B) but a drastic reduction in infectivity (Fig. 2C). We further examined the cause of this phenotype by designing individual substitutions. Mutants $P_{176}A$ and $E_{177}A$ exhibited no defect in replication and slight reductions in infectivity. However, mutant $I_{178}A$ showed a slight delay in RNA replication but a profound (>10,000-fold) reduction in infectivity (Fig. 2D and E). The absence of major defects in replication by changing each residue of the linker supports the hypothesis that this region is only marginally implicated in NS3 enzymatic activities but plays an important role in infectious particle production, presumably by modulating overall NS3 conformation. The delay in replication of the $I_{178}A$ mutant is in agreement with the functional shortage observed in DENV-4 NS3 linker mutants that increased protein flexibility (50). Our results are consistent with the idea that flexibility of the linker contributes to modulating the multifunctional activities of NS3, likely through allosteric interactions.

To complete a systematic analysis, we also examined a possible role of the NS3 protease domain in viral infectivity, which has never been explored before for viral assembly. Structure-based mutations were designed to substitute alanine for solvent-exposed side chain residues, avoiding those included in catalytic motifs (Fig. 3A). The solvent-accessible surface area for each residue within the NS3 protease domain was calculated from the X-ray crystal structure of the NS2B-NS3 protease domain (PDB code 2FOM). Seven double-residue mutants were designed and constructed in the context of the mDV-R system. Overall, the mutated sites were distributed evenly over the surface of NS3pro, as depicted in Fig. 3B. In addition, a mutation that replaced two proline residues in a proline-rich region at the intrinsically unstructured N-terminal region of the NS3 protein was also included (53).

Mutants $E_{88}A+K_{90}A$ and $K_{142}A+K_{143}A$ showed replication and infectivity levels similar to those of the WT (Fig. 3C and D). Mutant $P_{102}A+K_{104}A$ exhibited a drastic reduction in luciferase levels similar to that of the NS5 control, indicating that these residues are critical for DENV-2 replication. Mutant $K_{117}A+N_{119}A$ showed a significant reduction in viral replication and, probably as a consequence of this, a major reduction in virus production/infectivity (Fig. 3C). Mutant $R_{157}A+S_{158}A$ exhibited no defect in replication but an ~100-fold decrease in infectivity (Fig. 3C). Unexpectedly, mutants $P_{10}A+P_{12}A$ and $K_{63}A+R_{64}A$ exhibited no defect in viral replication, but infectious particle formation was almost abolished (Fig. 3C). We then designed the single-residue mutants $P_{10}A$, $P_{12}A$, $K_{63}A$, and $R_{64}A$ and extended the analysis to include single substitutions within the uncharacterized Pro-rich N terminus of the protease domain, residues 4 to 12 (Fig. 3E). With the exception of L_4A, none of the mutants exhibited a defect in viral replication, with luciferase activity levels similar to those of the WT at 6, 24, 48, and 72 h (Fig. 3F). Interestingly, a wide variety of phenotypes in the production of infectious particles was observed (Fig. 3G). S_9A and $P_{12}A$ mutations showed no apparent defect in infectivity, $K_{63}A$ displayed a minor reduction, P_8A, $P_{11}A$, and $R_{64}A$ exhibited a significant decrease, and L_4A, W_5A, D_6A, V_7A and $P_{10}A$ abolished infectious particle formation (Fig. 3G). Our results support a novel role of the N-terminal region of the NS3 protease domain on infectious viral particle release without participating in early viral replication steps. This finding supports the hypothesis that the structurally disordered N-terminal region of NS3 does not modulate protein enzymatic activities but rather participates in viral assembly.

We defined novel functions of the N-terminal region and the interdomain linker of DENV NS3 on production of infectious particles using a reporter system that allowed us to focus on mutant viruses fully competent for translation and RNA replication. Since this is the first study reporting a role of different domains of NS3 on DENV particle assembly, we further investigated phenotypic properties of these mutant viruses in the context of the infectious 16681 strain of DENV-2. We selected mutants that were competent for replication with substitutions in the N-terminal, protease, linker, and helicase domains and incorporated each one in the infectious cDNA clone.

Viruses containing the individual W_5A, D_6A, V_7A, $P_{10}A$, $I_{178}A$, or $N_{576}A$ mutation were constructed, and transcribed vRNAs were transfected into BHK-21 cells in parallel with controls (Fig. 4A). Two days after transfection, cells were examined by immunofluorescence assay (IFA) using anti-E monoclonal antibody. A similar signal of the viral protein was observed for WT and mutant viruses at 2 days posttransfection (Fig. 4A, vRNA transfections), suggesting that the mutations did not affect early steps of viral translation/replication as expected. Subsequently, viral infectivity from the supernatant media collected 2 dpt was evaluated by IFA at 1 and 4 days postincubation of fresh BHK-21 cells (Fig. 4A, infections). Consistent with the results obtained with the reporter virus, a dramatic decrease in viral spread in all mutants as a consequence of single-point mutations in NS3 was observed. The only mutant that showed a low but detectable level of propagation was the $N_{576}A$ mutation, which displayed merely 1% of the monolayer positive signal for the viral antigen (Fig. 4A).

To rule out that the infectivity impairment of the NS3 mutants was due to a defect in proteolytic processing of the viral polyprotein that unexpectedly impacted viral assembly or protein stabil-

FIG 3 Proline-rich N-terminal region of the NS3 protease domain is a novel determinant for DENV infectious particle formation. (A) Sequence of the N-terminal region of DENV-2 NS3 comprising the protease domain (residues 1 to 169). Conserved motifs of chymotrypsin-like protease are indicated in boxes. The mutated residues are shown in red. The interdomain linker region is highlighted in green. (B) Ribbon representation of the X-ray crystal structure of the protease domain of DENV-2 NS3 protein generated using Pymol (DeLano Scientific). The N-terminal third of the NS3 polypeptide, in orange, together with part of NS2B, in yellow, form the protease domain. The helicase domain is partially shown (in blue). The interdomain region (residues 170 to 178) is indicated in green. Double-residue mutations are indicated in red. The 18 residues of the unstructured N-terminal region of the protease domain are depicted as a dashed line. (C) Translation and replication capabilities of the luciferase reporter system mDV-R containing mutations in the protease domain of NS3 protein. Rluc activity was measured as a function of time after transfection in BHK-21 cells of genomic RNAs. WT reporter virus and controls were also included as indicated in the legend to Fig. 1. Data correspond to averages from three experiments. Error bars point out standard deviations. The dashed line indicates background levels of signal. (D) Released infectivity from mDV-R-transfected cells. Culture supernatants collected at 72 h posttransfection from DV-R RNA-transfected cells shown in panel C were used to infect fresh cells, and then luciferase activity in these cells was measured at 1 and 3 days postinfection. (E) Multiple-sequence alignment of the NS3 protease from flaviviruses showing the N-terminal region (left, residues 1 to 25) and a beta-hairpin region (right, residues 53 to 75). The double mutation of P_{10} and P_{12} as well as K_{63} and R_{64} (highlighted in gray) for alanine residues abrogated the release infectivity of reporter virus. (F) Translation and replication capabilities of the reporter viruses that carry a single-residue replacement of L_4A, W_5A, D_6A, V_7A, P_8A, S_9A, $P_{10}A$, $P_{11}A$, $P_{12}A$, $K_{63}A$, and $R_{64}A$ in RNA-transfected BHK-21 cells. (G) Release infectivity of the culture supernatants collected at 72 h posttransfection from DV-R RNA-transfected cells shown in panel F.

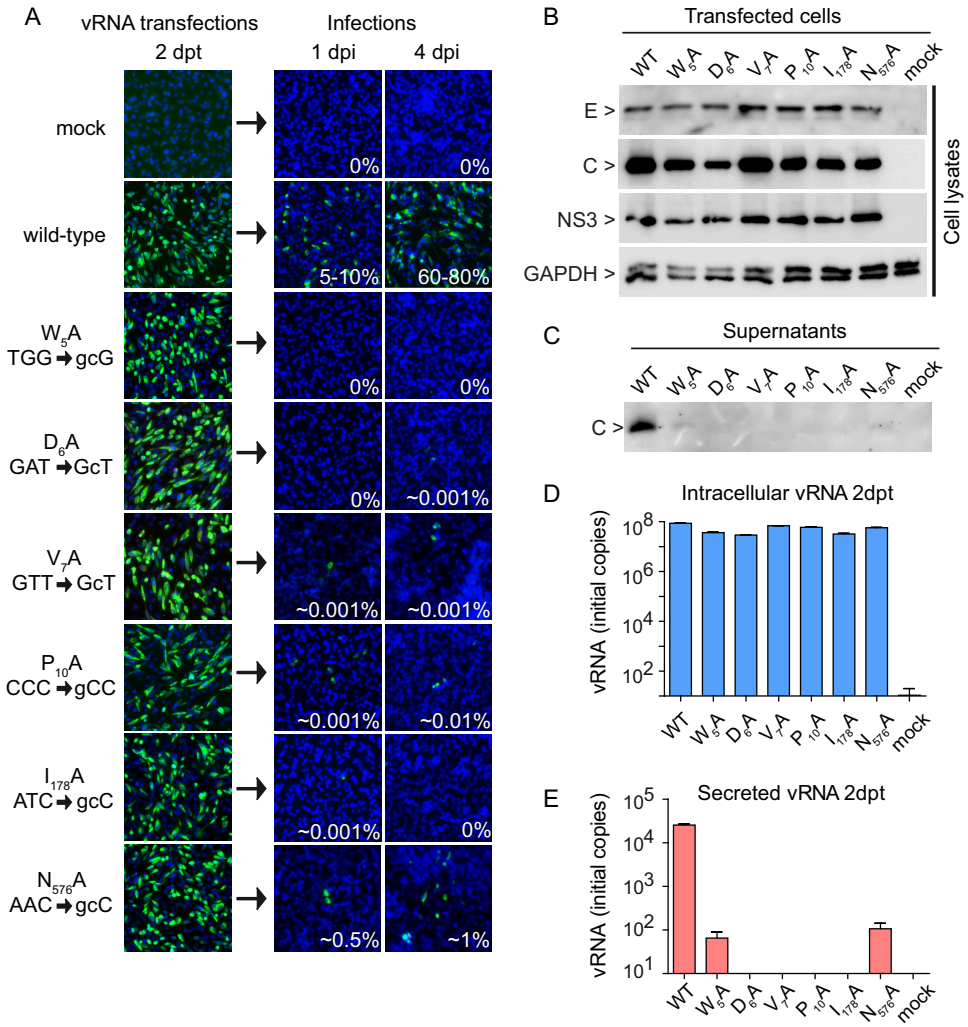

FIG 4 Multiple domains within NS3 are involved in assembly/secretion of DENV particles. (A) Representative images for IFA showing DENV antigen-positive BHK cells transfected with WT or mutant DENV-2 RNAs at 2 days posttransfection. Culture supernatants and cells were harvested separately and stored at −70°C until use. Culture supernatants were thawed and applied to fresh cells to determine the viral propagation capabilities. Representative IFAs from 1 and 4 days postinfection are shown. Percentages of infected cells were determined in each case. (B) WBs from cell lysates for E, NS3, and C. Viral protein production in transfected cells at 2 dpt with mutated virus impaired in secreted infectivity is shown. GAPDH was utilized as a loading control. (C) WBs for detection of secreted C released to the extracellular milieu from transfected cells at 3 dpt. (D) RT-qPCR of cell lysates at 2 dpt to determine the intracellular amount of vRNA. (E) RT-qPCR to determine the secreted amount of vRNA released to the supernatant fluids from RNA-transfected cells at 2 dpt.

ity, Western blot analyses against C, E, and NS3 proteins were performed for each mutant. Cell lysates collected at 2 dpt revealed comparable levels of viral proteins (Fig. 4B), confirming unaffected viral translation and polyprotein processing in the context of the infectious DENV clone. It is possible that noninfectious viral particles were secreted that were undetectable in a functional infection assay (Fig. 4A). If this were the case, inactive particles containing nucleocapsids (C and viral genome) would be secreted. To evaluate this possibility, both C and viral RNA were evaluated in the supernatants. Western blot assays were performed to detect C released in the media of transfected cells at 2 days posttransfection. While the WT virus showed strong accumulation of C and the mutants W_5A and $N_{576}A$ showed a faint band, C was undetectable in the media of cells transfected with the other mutants (Fig. 4C). To further confirm this observation, quantitative real-time RT-PCR was performed to determine the levels of intracellular and secreted viral RNA. To analyze the intracellular compartment, cells at 2 dpt were thoroughly washed with PBS and then total RNA was extracted. For the analysis of extracellular vRNA, culture fluids were collected and centrifuged for 15 min at 15,000 × *g*, and then supernatants were used for RNA extraction. As shown in Fig. 4D, similar amounts of viral RNA were observed in the intracellular compartments of transfected cells for the WT and all NS3 mutants, confirming that RNA replication and stability were not significantly affected by NS3 mutations. In contrast, the amounts of vRNA in the extracellular media were drastically reduced for all of the mutant viruses >1,000-fold, consistent with impaired secretion of infectious particles (Fig. 4E). Again, vRNA was detectable for the W_5A and the $N_{576}A$ mutants.

Because W_5A and $N_{576}A$ were mutants that displayed a highly reduced but detectable secreted vRNA (Fig. 4E), we further characterized these viruses. Growth curves were performed comparing

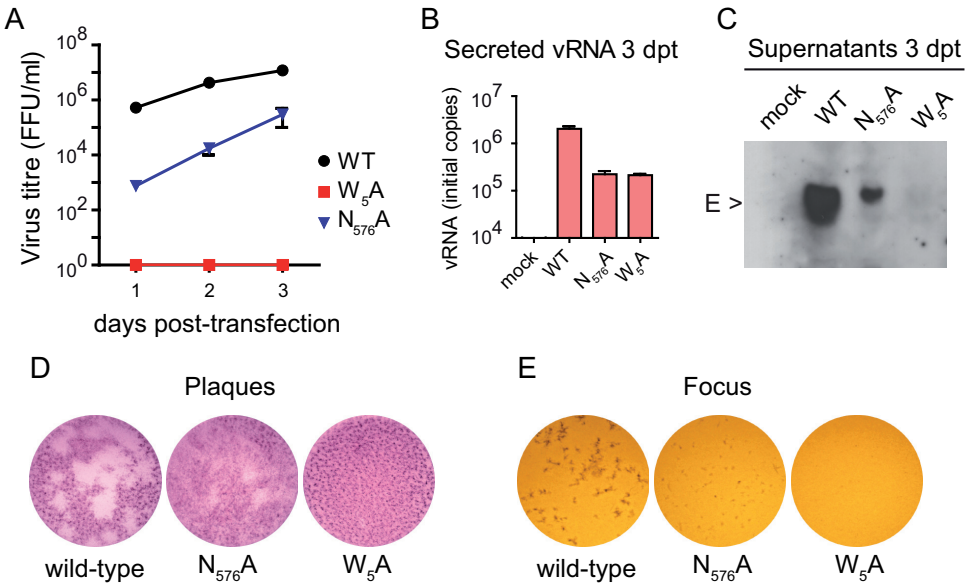

FIG 5 Characterization of selected NS3 mutants defective in propagation reveals singular deficiencies. (A) Focus-forming unit (FFU) quantification by serial dilution titrations of supernatants collected for each virus at the indicated time posttransfection. (B) Secreted vRNA was analyzed by RT-qPCR. Total RNA was extracted from supernatant fluids of transfected cells collected at 3 dpt and reverse transcribed prior to being assayed by qPCR. (C) Secreted E protein was analyzed by WB. Supernatant fluids of transfected cells collected at 3 dpt were applied to SDS-PAGE followed by WB. (D) Virus PFU were analyzed from culture supernatants from WT and $N_{576}A$ and W_5A mutant vRNA-transfected cells. WT virus produced well-defined plaques, whereas $N_{576}A$ produced tiny and diffuse plaques. No plaques were detected for W_5A virus. (E) Viral focus-forming units were immunodetected for the WT and $N_{576}A$ mutant, although those of the latter were of a smaller size. No FFU were detected for W_5A.

their replication to that of the WT (Fig. 5A). The growth curve demonstrates an increase of $N_{576}A$ mutant approaching the WT level from day 1 to day 3 (about 1,000-, 400-, and 100-fold lower titers in supernatant fluids collected at 1, 2, and 3 dpt, respectively). This mutant virus approaches the WT level because the WT reaches its maximum at about 3 days posttransfection while the mutant continues replicating. This observation is compatible with the reduction in vRNA detected in the supernatants by quantitative real-time RT-PCR (Fig. 4E and 5B). In addition, a reduced level of released E protein was observed for this mutant compared to the WT in supernatants at 3 dpt (Fig. 5C). Furthermore, although detectable, this mutant displayed small and diffuse plaques and small infectious focus phenotypes, as observed in virus plaque- and focus-forming assays (Fig. 5D and E, respectively). The results are consistent with the idea that mutation $N_{576}A$ largely reduces the amount of particles produced but the virions released are infectious.

Mutant W_5A was particularly interesting because it did not propagate in any of the functional assays tested (IFA and virus plaque- and focus-forming assays in Fig. 4A and 5A, D, and E), but vRNA and C were detected in the media of transfected cells (Fig. 4C and E and 5B). The secreted vRNA at 3 dpi was only 20-fold lower than that of the WT, but the E protein was undetectable (Fig. 5B and C). These observations are consistent with the idea that vRNA was secreted at low levels by a noncanonical process, possibly as naked nucleocapsids that were not infectious. This was different from that observed for mutant $N_{576}A$, in which every parameter analyzed was consistent with very low levels of infectious particle secretion.

Taking these findings together, we conclude that mutants in the NS3 protein do not release significant amounts of noninfectious particles and the defects observed are associated with particle formation or release. Interestingly, we identified a novel proline-rich, N-terminal region of the DENV NS3 protease domain as a determinant for production of infectious viral particles. Sequence analyses of this region revealed that it is highly conserved among different flaviviruses, and structural analysis supports the conservation of an intrinsically unstructured region.

We did not expect to find determinants for DENV assembly in separate regions of the large NS3 protein. We speculate that NS3 serves as a platform for interactions with viral and/or host factors implicated in the production of infectious particles. In this regard, proteolytic cleavage of capsid from the viral polyprotein by NS2B3 has been proposed to be coordinated with nucleocapsid assembly and uptake of the complex into budding particles (54). Thus, it is possible that the presence of NS3, acting as a protease for capsid maturation, also performs a function in coordinating genome recruitment. This is also relevant when taking into account that NS3 is in intimate interaction with the viral genome during RNA replication, acting as an RNA helicase and RNA annealing enzyme. Here, we provide direct evidence for the involvement of different domains of NS3 in viral particle formation. Because the flavivirus machinery for the initial steps of particle assembly still is unknown, our work provides a framework to further explore NS3 participation. The definition of the NS3 protein-protein interaction network with host and viral proteins will be the next step to dissect the components and mechanism of viral particle assembly.

ACKNOWLEDGMENTS

We thank members of the Gamarnik laboratory for helpful discussions.

A.V.G., L.G.G., C.V.F., and N.G.I. are members of the Argentinean Council of Investigation (CONICET).

This work was supported by NIH (NIAID) grants R01.AI095175 and PICT-2014-2111. L.B. and F.A.D. were granted CONICET fellowships.

FUNDING INFORMATION

This work, including the efforts of Andrea Gamarnik, was funded by National Institutes of Health (NIH) (R01.AI095175). This work, including the efforts of Andrea Gamarnik, was funded by National Agency for Promotion of Science Argentina (PICT-2014-2111).

REFERENCES

1. **Musso D, Cao-Lormeau VM, Gubler DJ.** 2015. Zika virus: following the path of dengue and chikungunya? Lancet **386:**243–244. http://dx.doi.org/10.1016/S0140-6736(15)61273-9.
2. **Lindenbach BD, Murray CL, Thiel HJ, Rice CD.** 2013. Flaviviridae: the viruses and their replication, p 712–746. *In* Knipe DM, Howley PM, Cohen JI, Griffin DE, Lamb RA, Martin MA, Racaniello VR, Roizman B (ed), Fields virology, vol 1. Lippincott-Raven, Philadelphia, PA.
3. **Pierson TC, Diamond MS.** 2013. Flaviviruses, p 747–794. *In* Knipe DM, Howley PM, Cohen JI, Griffin DE, Lamb RA, Martin MA, Racaniello VR, Roizman B (ed), Fields virology, vol 1. Lippincott-Raven, Philadelphia, PA.
4. **Bhatt S, Gething PW, Brady OJ, Messina JP, Farlow AW, Moyes CL, Drake JM, Brownstein JS, Hoen AG, Sankoh O, Myers MF, George DB, Jaenisch T, Wint GR, Simmons CP, Scott TW, Farrar JJ, Hay SI.** 2013. The global distribution and burden of dengue. Nature **496:**504–507. http://dx.doi.org/10.1038/nature12060.
5. **Sampath A, Padmanabhan R.** 2009. Molecular targets for flavivirus drug discovery. Antiviral Res **81:**6–15. http://dx.doi.org/10.1016/j.antiviral.2008.08.004.
6. **Filomatori CV, Iglesias NG, Villordo SM, Alvarez DE, Gamarnik AV.** 2011. RNA sequences and structures required for the recruitment and activity of the dengue virus polymerase. J Biol Chem **286:**6929–6939. http://dx.doi.org/10.1074/jbc.M110.162289.
7. **Ackermann M, Padmanabhan R.** 2001. De novo synthesis of RNA by the dengue virus RNA-dependent RNA polymerase exhibits temperature dependence at the initiation but not elongation phase. J Biol Chem **276:**39926–39937. http://dx.doi.org/10.1074/jbc.M104248200.
8. **Ashour J, Laurent-Rolle M, Shi PY, Garcia-Sastre A.** 2009. NS5 of dengue virus mediates STAT2 binding and degradation. J Virol **83:**5408–5418. http://dx.doi.org/10.1128/JVI.02188-08.
9. **Le Breton M, Meyniel-Schicklin L, Deloire A, Coutard B, Canard B, de Lamballerie X, Andre P, Rabourdin-Combe C, Lotteau V, Davoust N.** 2011. Flavivirus NS3 and NS5 proteins interaction network: a high-throughput yeast two-hybrid screen. BMC Microbiol **11:**234. http://dx.doi.org/10.1186/1471-2180-11-234.
10. **Morrison J, Laurent-Rolle M, Maestre AM, Rajsbaum R, Pisanelli G, Simon V, Mulder LC, Fernandez-Sesma A, Garcia-Sastre A.** 2013. Dengue virus co-opts UBR4 to degrade STAT2 and antagonize type I interferon signaling. PLoS Pathog **9:**e1003265. http://dx.doi.org/10.1371/journal.ppat.1003265.
11. **Tay MY, Saw WG, Zhao Y, Chan KW, Singh D, Chong Y, Forwood JK, Ooi EE, Gruber G, Lescar J, Luo D, Vasudevan SG.** 2015. The C-terminal 50 amino acid residues of dengue NS3 protein are important for NS3-NS5 interaction and viral replication. J Biol Chem **290:**2379–2394. http://dx.doi.org/10.1074/jbc.M114.607341.
12. **Alvarez DE, Lodeiro MF, Luduena SJ, Pietrasanta LI, Gamarnik AV.** 2005. Long-range RNA-RNA interactions circularize the dengue virus genome. J Virol **79:**6631–6643. http://dx.doi.org/10.1128/JVI.79.11.6631-6643.2005.
13. **Filomatori CV, Lodeiro MF, Alvarez DE, Samsa MM, Pietrasanta L, Gamarnik AV.** 2006. A 5′ RNA element promotes dengue virus RNA synthesis on a circular genome. Genes Dev **20:**2238–2249. http://dx.doi.org/10.1101/gad.1444206.
14. **Selisko B, Wang C, Harris E, Canard B.** 2014. Regulation of flavivirus RNA synthesis and replication. Curr Opin Virol **9:**74–83. http://dx.doi.org/10.1016/j.coviro.2014.09.011.
15. **Clyde K, Harris E.** 2006. RNA secondary structure in the coding region of dengue virus type 2 directs translation start codon selection and is required for viral replication. J Virol **80:**2170–2182. http://dx.doi.org/10.1128/JVI.80.5.2170-2182.2006.
16. **Khromykh AA, Meka H, Guyatt KJ, Westaway EG.** 2001. Essential role of cyclization sequences in flavivirus RNA replication. J Virol **75:**6719–6728. http://dx.doi.org/10.1128/JVI.75.14.6719-6728.2001.
17. **Khromykh AA, Varnavski AN, Sedlak PL, Westaway EG.** 2001. Coupling between replication and packaging of flavivirus RNA: evidence derived from the use of DNA-based full-length cDNA clones of Kunjin virus. J Virol **75:**4633–4640. http://dx.doi.org/10.1128/JVI.75.10.4633-4640.2001.
18. **Welsch S, Miller S, Romero-Brey I, Merz A, Bleck CK, Walther P, Fuller SD, Antony C, Krijnse-Locker J, Bartenschlager R.** 2009. Composition and three-dimensional architecture of the dengue virus replication and assembly sites. Cell Host Microbe **5:**365–375. http://dx.doi.org/10.1016/j.chom.2009.03.007.
19. **Apte-Sengupta S, Sirohi D, Kuhn RJ.** 2014. Coupling of replication and assembly in flaviviruses. Curr Opin Virol **9:**134–142. http://dx.doi.org/10.1016/j.coviro.2014.09.020.
20. **Liu WJ, Sedlak PL, Kondratieva N, Khromykh AA.** 2002. Complementation analysis of the flavivirus Kunjin NS3 and NS5 proteins defines the minimal regions essential for formation of a replication complex and shows a requirement of NS3 in cis for virus assembly. J Virol **76:**10766–10775. http://dx.doi.org/10.1128/JVI.76.21.10766-10775.2002.
21. **Gillespie LK, Hoenen A, Morgan G, Mackenzie JM.** 2010. The endoplasmic reticulum provides the membrane platform for biogenesis of the flavivirus replication complex. J Virol **84:**10438–10447. http://dx.doi.org/10.1128/JVI.00986-10.
22. **Kummerer BM, Rice CM.** 2002. Mutations in the yellow fever virus nonstructural protein NS2A selectively block production of infectious particles. J Virol **76:**4773–4784. http://dx.doi.org/10.1128/JVI.76.10.4773-4784.2002.
23. **Patkar CG, Kuhn RJ.** 2008. Yellow fever virus NS3 plays an essential role in virus assembly independent of its known enzymatic functions. J Virol **82:**3342–3352. http://dx.doi.org/10.1128/JVI.02447-07.
24. **Scaturro P, Cortese M, Chatel-Chaix L, Fischl W, Bartenschlager R.** 2015. Dengue virus non-structural protein 1 modulates infectious particle production via interaction with the structural proteins. PLoS Pathog **11:**e1005277. http://dx.doi.org/10.1371/journal.ppat.1005277.
25. **Vossmann S, Wieseler J, Kerber R, Kummerer BM.** 2015. A basic cluster in the N terminus of yellow fever virus NS2A contributes to infectious particle production. J Virol **89:**4951–4965. http://dx.doi.org/10.1128/JVI.03351-14.
26. **Xie X, Gayen S, Kang C, Yuan Z, Shi PY.** 2013. Membrane topology and function of dengue virus NS2A protein. J Virol **87:**4609–4622. http://dx.doi.org/10.1128/JVI.02424-12.
27. **Leung JY, Pijlman GP, Kondratieva N, Hyde J, Mackenzie JM, Khromykh AA.** 2008. Role of nonstructural protein NS2A in flavivirus assembly. J Virol **82:**4731–4741. http://dx.doi.org/10.1128/JVI.00002-08.
28. **Wengler G, Czaya G, Farber PM, Hegemann JH.** 1991. In vitro synthesis of West Nile virus proteins indicates that the amino-terminal segment of the NS3 protein contains the active centre of the protease which cleaves the viral polyprotein after multiple basic amino acids. J Gen Virol **72**(Part 4)**:**851–858. http://dx.doi.org/10.1099/0022-1317-72-4-851.
29. **Chambers TJ, Grakoui A, Rice CM.** 1991. Processing of the yellow fever virus nonstructural polyprotein: a catalytically active NS3 proteinase domain and NS2B are required for cleavages at dibasic sites. J Virol **65:**6042–6050.
30. **Chambers TJ, Nestorowicz A, Rice CM.** 1995. Mutagenesis of the yellow fever virus NS2B/3 cleavage site: determinants of cleavage site specificity and effects on polyprotein processing and viral replication. J Virol **69:**1600–1605.
31. **Chambers TJ, Weir RC, Grakoui A, McCourt DW, Bazan JF, Fletterick RJ, Rice CM.** 1990. Evidence that the N-terminal domain of nonstructural protein NS3 from yellow fever virus is a serine protease responsible for site-specific cleavages in the viral polyprotein. Proc Natl Acad Sci U S A **87:**8898–8902. http://dx.doi.org/10.1073/pnas.87.22.8898.
32. **Benarroch D, Selisko B, Locatelli GA, Maga G, Romette JL, Canard B.** 2004. The RNA helicase, nucleotide 5′-triphosphatase, and RNA 5′-triphosphatase activities of Dengue virus protein NS3 are Mg2+-dependent and require a functional Walker B motif in the helicase catalytic core. Virology **328:**208–218. http://dx.doi.org/10.1016/j.virol.2004.07.004.
33. **Falgout B, Pethel M, Zhang YM, Lai CJ.** 1991. Both nonstructural proteins NS2B and NS3 are required for the proteolytic processing of dengue virus nonstructural proteins. J Virol **65:**2467–2475.
34. **Matusan AE, Pryor MJ, Davidson AD, Wright PJ.** 2001. Mutagenesis of

the dengue virus type 2 NS3 protein within and outside helicase motifs: effects on enzyme activity and virus replication. J Virol **75:**9633–9643. http://dx.doi.org/10.1128/JVI.75.20.9633-9643.2001.

35. **Liu WJ, Chen HB, Khromykh AA.** 2003. Molecular and functional analyses of Kunjin virus infectious cDNA clones demonstrate the essential roles for NS2A in virus assembly and for a nonconservative residue in NS3 in RNA replication. J Virol **77:**7804–7813. http://dx.doi.org/10.1128/JVI.77.14.7804-7813.2003.
36. **Pijlman GP, Kondratieva N, Khromykh AA.** 2006. Translation of the flavivirus Kunjin NS3 gene in cis but not its RNA sequence or secondary structure is essential for efficient RNA packaging. J Virol **80:**11255–11264. http://dx.doi.org/10.1128/JVI.01559-06.
37. **Westaway EG, Mackenzie JM, Kenney MT, Jones MK, Khromykh AA.** 1997. Ultrastructure of Kunjin virus-infected cells: colocalization of NS1 and NS3 with double-stranded RNA, and of NS2B with NS3, in virus-induced membrane structures. J Virol **71:**6650–6661.
38. **Aguirre S, Maestre AM, Pagni S, Patel JR, Savage T, Gutman D, Maringer K, Bernal-Rubio D, Shabman RS, Simon V, Rodriguez-Madoz JR, Mulder LC, Barber GN, Fernandez-Sesma A.** 2012. DENV inhibits type I IFN production in infected cells by cleaving human STING. PLoS Pathog **8:**e1002934. http://dx.doi.org/10.1371/journal.ppat.1002934.
39. **Yu CY, Chang TH, Liang JJ, Chiang RL, Lee YL, Liao CL, Lin YL.** 2012. Dengue virus targets the adaptor protein MITA to subvert host innate immunity. PLoS Pathog **8:**e1002780. http://dx.doi.org/10.1371/journal.ppat.1002780.
40. **Gebhard LG, Kaufman SB, Gamarnik AV.** 2012. Novel ATP-independent RNA annealing activity of the dengue virus NS3 helicase. PLoS One **7:**e36244. http://dx.doi.org/10.1371/journal.pone.0036244.
41. **Incicco JJ, Gebhard LG, Gonzalez-Lebrero RM, Gamarnik AV, Kaufman SB.** 2013. Steady-state NTPase activity of dengue virus NS3: number of catalytic sites, nucleotide specificity and activation by ssRNA. PLoS One **8:**e58508. http://dx.doi.org/10.1371/journal.pone.0058508.
42. **Li H, Clum S, You S, Ebner KE, Padmanabhan R.** 1999. The serine protease and RNA-stimulated nucleoside triphosphatase and RNA helicase functional domains of dengue virus type 2 NS3 converge within a region of 20 amino acids. J Virol **73:**3108–3116.
43. **Samsa MM, Mondotte JA, Iglesias NG, Assuncao-Miranda I, Barbosa-Lima G, Da Poian AT, Bozza PT, Gamarnik AV.** 2009. Dengue virus capsid protein usurps lipid droplets for viral particle formation. PLoS Pathog **5:**e1000632. http://dx.doi.org/10.1371/journal.ppat.1000632.
44. **Kinney RM, Butrapet S, Chang GJ, Tsuchiya KR, Roehrig JT, Bhamarapravati N, Gubler DJ.** 1997. Construction of infectious cDNA clones for dengue 2 virus: strain 16681 and its attenuated vaccine derivative, strain PDK-53. Virology **230:**300–308. http://dx.doi.org/10.1006/viro.1997.8500.
45. **Alvarez DE, De Lella Ezcurra AL, Fucito S, Gamarnik AV.** 2005. Role of RNA structures present at the 3′UTR of dengue virus on translation, RNA synthesis, and viral replication. Virology **339:**200–212. http://dx.doi.org/10.1016/j.virol.2005.06.009.
46. **Samsa MM, Mondotte JA, Caramelo JJ, Gamarnik AV.** 2012. Uncoupling cis-acting RNA elements from coding sequences revealed a requirement of the N-terminal region of dengue virus capsid protein in virus particle formation. J Virol **86:**1046–1058. http://dx.doi.org/10.1128/JVI.05431-11.
47. **Oliphant T, Engle M, Nybakken GE, Doane C, Johnson S, Huang L, Gorlatov S, Mehlhop E, Marri A, Chung KM, Ebel GD, Kramer LD, Fremont DH, Diamond MS.** 2005. Development of a humanized monoclonal antibody with therapeutic potential against West Nile virus. Nat Med **11:**522–530. http://dx.doi.org/10.1038/nm1240.
48. **Xu T, Sampath A, Chao A, Wen D, Nanao M, Chene P, Vasudevan SG, Lescar J.** 2005. Structure of the Dengue virus helicase/nucleoside triphosphatase catalytic domain at a resolution of 2.4 A. J Virol **79:**10278–10288. http://dx.doi.org/10.1128/JVI.79.16.10278-10288.2005.
49. **Fraczkiewicz R, Braun W.** 1998. Exact and efficient analytical calculation of the accessible surface areas and their gradients for macromolecules. J Comput Chem **19:**319–333.
50. **Luo D, Wei N, Doan DN, Paradkar PN, Chong Y, Davidson AD, Kotaka M, Lescar J, Vasudevan SG.** 2010. Flexibility between the protease and helicase domains of the dengue virus NS3 protein conferred by the linker region and its functional implications. J Biol Chem **285:**18817–18827.
51. **Assenberg R, Mastrangelo E, Walter TS, Verma A, Milani M, Owens RJ, Stuart DI, Grimes JM, Mancini EJ.** 2009. Crystal structure of a novel conformational state of the flavivirus NS3 protein: implications for polyprotein processing and viral replication. J Virol **83:**12895–12906. http://dx.doi.org/10.1128/JVI.00942-09.
52. **Luo D, Xu T, Hunke C, Gruber G, Vasudevan SG, Lescar J.** 2008. Crystal structure of the NS3 protease-helicase from dengue virus. J Virol **82:**173–183. http://dx.doi.org/10.1128/JVI.01788-07.
53. **Erbel P, Schiering N, D'Arcy A, Renatus M, Kroemer M, Lim SP, Yin Z, Keller TH, Vasudevan SG, Hommel U.** 2006. Structural basis for the activation of flaviviral NS3 proteases from dengue and West Nile virus. Nat Struct Mol Biol **13:**372–373. http://dx.doi.org/10.1038/nsmb1073.
54. **Lobigs M, Lee E, Ng ML, Pavy M, Lobigs P.** 2010. A flavivirus signal peptide balances the catalytic activity of two proteases and thereby facilitates virus morphogenesis. Virology **401:**80–89. http://dx.doi.org/10.1016/j.virol.2010.02.008.